Ultramicroscopy 110 (2010) 682–688

Contents lists available at ScienceDirect

Ultramicroscopy

journal homepage: www.elsevier.com/locate/ultramic

Molecular dynamics of DNA and nucleosomes in solution studied by fast-scanning atomic force microscopy

Yuki Suzuki [a,*], Yuji Higuchi [b], Kohji Hizume [a], Masatoshi Yokokawa [a], Shige H. Yoshimura [a], Kenichi Yoshikawa [b], Kunio Takeyasu [a]

[a] Laboratory of Plasma Membrane and Nuclear Signaling, Graduate School of Biostudies, Kyoto University, Yoshida-Konoe-cho, Sakyo-ku, Kyoto 606-8501, Japan
[b] Department of Physics, Graduate School of Science, Kyoto University, Kita-shirakawa Oiwake-cho, Sakyo-ku, Kyoto 606-8502, Japan

ARTICLE INFO

Keywords:
Atomic force microscopy
Fast-scanning atomic force microscopy
Nucleosome
Chromatin
Histone

ABSTRACT

Nucleosome is a fundamental structural unit of chromatin, and the exposure from or occlusion into chromatin of genomic DNA is closely related to the regulation of gene expression. In this study, we analyzed the molecular dynamics of poly-nucleosomal arrays in solution by fast-scanning atomic force microscopy (AFM) to obtain a visual glimpse of nucleosome dynamics on chromatin fiber at single molecule level. The influence of the high-speed scanning probe on nucleosome dynamics can be neglected since bending elastic energy of DNA molecule showed similar probability distributions at different scan rates. In the sequential images of poly-nucleosomal arrays, the sliding of the nucleosome core particle and the dissociation of histone particle were visualized. The sliding showed limited fluctuation within ~50 nm along the DNA strand. The histone dissociation occurs by at least two distinct ways: a dissociation of histone octamer or sequential dissociations of tetramers. These observations help us to develop the molecular mechanisms of nucleosome dynamics and also demonstrate the ability of fast-scanning AFM for the analysis of dynamic protein–DNA interaction in sub-seconds time scale.

1. Introduction

Double helical DNA is the molecule that harbors genetic programs in cells. For the excursion of such programs, the physical properties of DNA are critical. DNA can be described as a semi-flexible chain, a coarse-grained model that depends on a persistence length of 50 nm (=150 bp) of DNA [1,2]. The elastic properties restrict writhing and twisting of DNA molecule, and thus superhelicity as a whole. Upon protein binding, further topological constraint can be imposed or superhelicity would be neutralized. These properties of DNA are critical in various steps of achieving higher-order structures; e.g., (i) loop formation between two distantly separated enhancer-binding sites on the DNA [3], (ii) nucleosome formation with core histone octamer [4], (iii) formation of Holiday Junction [5], and others. These higher-order structures are supposed to be important for the regulation of gene expression [6,7], restriction enzyme activity [8], site-specific recombination [9], and others. Indeed, a structural study has shown that a local strain imposed by initiator binding can induce a drastic shift of DNA conformation from a supercoiled to a relaxed state [10]. In this case, without introduction of a DNA strand break or a local melting of the DNA double strand, the superhelical strain of a closed circular DNA can be drastically redistributed over several kilobases from writhing to twisting upon protein binding, which, in turn, induces an apparent relaxation of circular DNA.

Eukaryotic genomic DNA interacts with a number of proteins and is folded into higher-order chromatin fibers through several hierarchical packaging. The most fundamental structural unit of chromatin is the nucleosome, which is composed of about 146 bp DNA wrapping ~1.75 turns around a histone octamer [11–13]. The nucleosome imposes a significant barrier for regulatory factors that control the process of gene expression [14]. A competitive protein-binding assay has demonstrated that nucleosomal DNA at the edge of nucleosome core particle is capable of unwrapping spontaneously [15,16]. This unwrapping likely provides an opportunity for proteins to bind nucleosomal DNA. Another dynamic property of nucleosome is sliding. It has been biochemically demonstrated that nucleosomes spontaneously reposition themselves along DNA when the temperature or the ionic strength of the solution increases [17–19]. A combination of a Brownian dynamics simulation and atomic force microscopy (AFM) has demonstrated that this sliding motion is caused by a manifestation of Brownian motion [20]. Single-molecule approaches have also been applied to analyze dynamic aspects of nucleosomes in the absence of remodeling factors. Single-molecule measurement using optical trap has shown that the wrapping and unwrapping of DNA between 1 and 1.75 turns occur reversibly

* Corresponding author. Tel./fax: +81 75 753 7906.
E-mail address: ysuzuki79.m07@lif.kyoto-u.ac.jp (Y. Suzuki).

0304-3991/$ - see front matter © 2010 Elsevier B.V. All rights reserved.
doi:10.1016/j.ultramic.2010.02.032

[21,22]. Single-molecule fluorescence resonance energy transfer (FRET) techniques have detected a local dissociation of DNA from histone core particle occurring in sub-second time scale [23,24]. These investigations indicate that thermal fluctuation is possibly responsible for the nucleosome dynamics.

The capability of AFM operating in solution has made it possible to study structural and mechanical properties of biological molecules under "physiological conditions" [25–29]. Newly developed fast-scanning AFMs have a miniaturized cantilever and scan stage to reduce the mechanical response time of the cantilever and to prevent the onset of resonant motion during high-speed scanning [30]. Fast temporal resolutions of 1–3 frames per second (fps) allow the dynamics of biomolecules to be followed more closely on the sub-second time scale [30–33]. Taking advantage of the fast-scanning AFM in spatial and temporal resolution, we applied this method to analyze the molecular dynamics of DNA and nucleosomes in solution. The motion of the plasmid DNA was followed at the scan rate of 1–3 fps. The analyses of bending elastic energy of DNA segments demonstrated that the movement of DNA was a reflection of thermal fluctuation, and that the movement of DNA molecule was little affected by the scanning probe. We were also able to visualize the morphological changes of nucleosomal array, accompanied with sliding or dissociation of histone core particle. Nucleosomes underwent two different dissociation pathways, resulting in release of the histone octamer or its constituents.

2. Material and methods

2.1. DNA and histones

The 3993 bp plasmid DNA pGEMEX-1 (Promega) was used for fast-scanning AFM analysis. The 1890 bp DNA fragment used in the chromatin reconstitution was derived from 2961 bp pBluescript II KS(-) by double digest at *ScaI* and *XhoI* sites.

Core histones were purified from HeLa cells according to the method developed by O'Neill et al. [14] with slight modifications [34].

2.2. Chromatin reconstitution and conventional AFM imaging

Equal amounts (0.5 μg) of the purified DNA and the histone octamer were mixed in Hi-buffer [10 mM Tris–Cl (pH 7.5), 2 M NaCl, 1 mM EDTA, 0.05% NP-40, and 5 mM β-mercaptoethanol], and placed in a dialysis tube (total volume 50 μl). The dialysis was started in 150 ml of Hi-buffer with stirring at 4 °C. Lo-buffer [10 mM Tris–Cl (pH 7.5), 1 mM EDTA, 0.05% NP-40, and 5 mM 2-mercaptoethanol] was added to the dialysis buffer at the rate of 0.46 ml/min, and the dialysis buffer was pumped out at the same rate with a peristaltic pump so that the final dialysis buffer contained 50 mM NaCl after 20 h. The sample was collected from the dialysis tube and stored at 4 °C until use.

For conventional AFM imaging using Digital Instruments Multi Mode AFM, the reconstituted chromatin solution was diluted to an appropriate concentration with buffer [5 mM HEPES–NaOH (pH 7.5), 50 mM NaCl]. The sample was dropped onto a freshly cleaved mica surface that had been pretreated with 10 mM spermidine. After 10 min incubation at room temperature, the mica was rinsed with water and dried under nitrogen gas.

All imaging was performed in air using the cantilever tapping mode. The cantilever (OMCL-AC160TS-W2, Olympus) was 129 μm in length with a spring constant of 33–62 N/m. The scanning frequency was 1–3 Hz, and images were captured using the height mode in a 512×512 pixel format. The obtained images were plane-fitted and flattened by the computer program supplied in the imaging module before analysis.

2.3. Fast-AFM observation

Two conflicting requirements generally have to be satisfied in the observation of molecular dynamics by AFM: (i) attachment of the molecules of interest onto the substrate surface and (ii) freedom of movement of the molecules. The molecules must retain enough mobility to allow dynamic movement. At the same time, the molecules must be stably adsorbed to the mica surface and remain within the scanning area during the imaging.

Since DNA and mica surface are both negatively charged in aqueous buffer, the condition for time-lapse imaging of DNA samples has been achieved by adjusting the concentration of Mg^{2+} [31,32]. The plasmid DNA pGEMEX-1 was diluted to a concentration of 1.0 ng/μl in a buffer containing 5 mM HEPES–NaOH (pH 7.5) and 2 mM $MgCl_2$, and 2 μl of the sample was immediately deposited onto freshly cleaved 1 mm^2 mica discs and incubated for 1 min. The sample was then rinsed with 2×10 μl washes of the buffer, and imaged in the same buffer.

For the observation of nucleosomal array, we avoided adding magnesium to the buffer, because divalent cation has strong effect on the interaction between nucleosomes and causes aggregates [35]. Instead, we used positively charged mica surface that had been treated with spermidine before sample deposition [34,36–38]. The reconstituted nucleosomal array was diluted to a concentration of 0.5 ng/μl in a buffer containing 5 mM HEPES–NaOH (pH 7.5) and 50 mM NaCl, and 3 μl of the sample was immediately deposited onto freshly cleaved 1 mm^2 mica discs pretreated with 10 mM spermidine. After 1 min incubation, the sample was rinsed with 2×10 μl washes of the buffer and then imaged in the same buffer without the drying step. One inevitable limitation of AFM imaging is the requirement of the sample to be bound to the mica surface. In the case of nucleosomes, the core histones tend to stick to the mica surface via spermidine, and this gives rise to a restriction against free movement of nucleosomes. Our experimental protocol permits us to investigate molecular dynamics of nucleosomes under this limited condition.

The AFM experiments were performed using a prototype high-speed AFM (see details in Refs. [31,33]). The sample was imaged in buffer solution at ambient temperature with a small cantilever of dimensions $L \times W \times H = 10 \times 2 \times 0.1$ μm^3 (Olympus Corporation, Tokyo, Japan). These cantilevers had a spring constant of 0.1–0.2 N/m with a resonant frequency in water of 400–1000 kHz and 192×144 pixel images were obtained at the scan rate of 1–3 fps. Individual frames of movie files were imported into Image J (http://rsb.info.nih.gov/ij/) and analyzed. Distances between nucleosomes were measured by tracing the contour length of DNA from the center of nucleosome to the center of adjacent nucleosome. The videos and images were provided in Adobe Photoshop CS3 to show only the molecules of interest (Fig. S1). For the analysis of volume, the "full-width at half-maximum" and height were measured with the fast-scanning AFM software and used for calculation as reported [39].

3. Results and discussion

3.1. Thermal fluctuation of DNA

Fig. 1A shows a series of consecutive images of a plasmid in solution captured at the scan rate of 1.0 fps. The DNA molecule showed swinging motions without breakage of the strand. Fluctuating motions of DNA strand on the mica surface were observed in both *x* and *y* directions, regardless of the experimental conditions that the scanning velocity was much greater along the *x*-axis (fast-scanning direction) than along the *y*-axis (slow-scanning direction; Fig. 1B). This indicates that the scanning

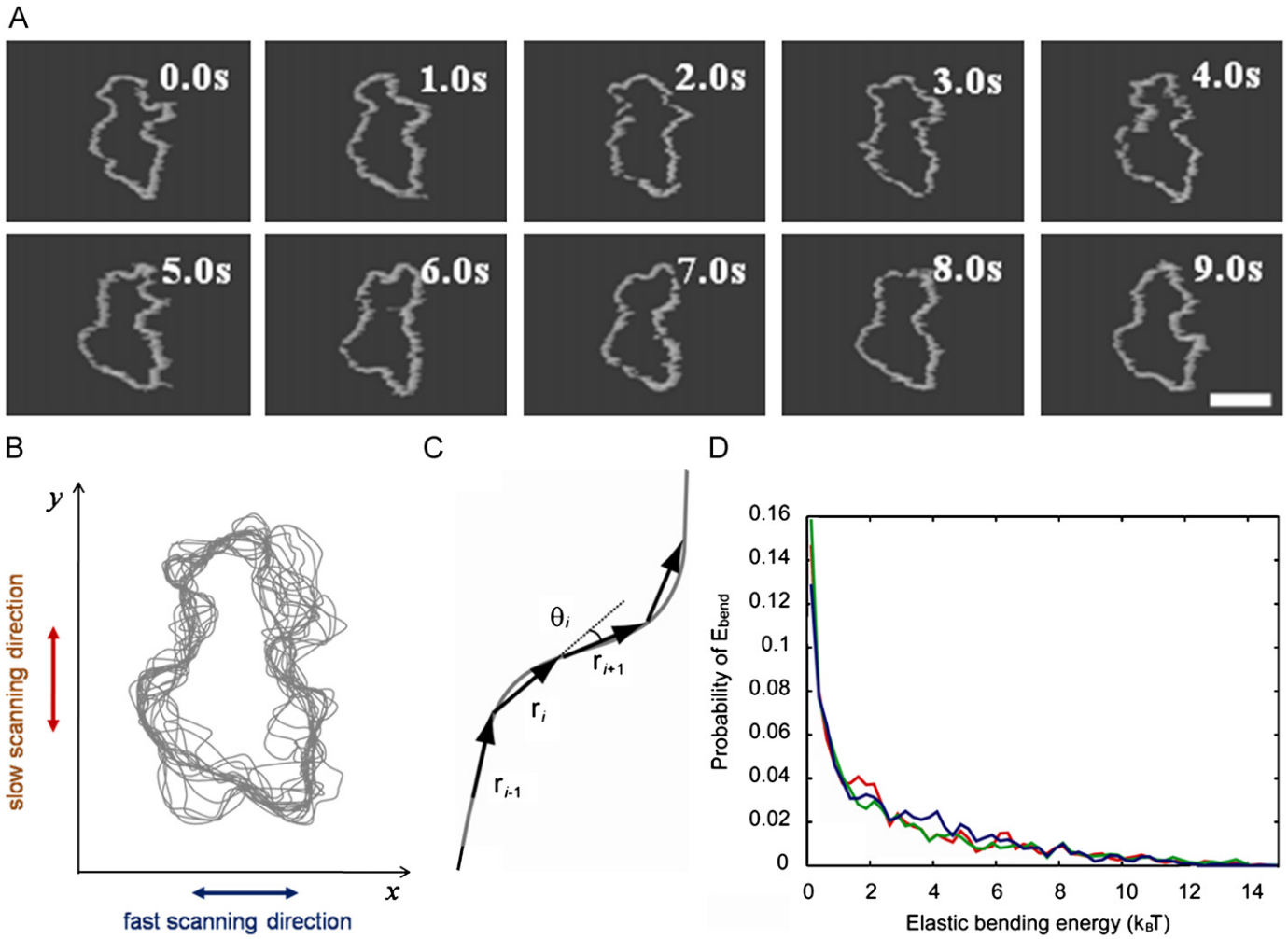

Fig. 1. Fast-scanning AFM analysis of the motion of plasmid DNA. (A) Successive time-lapse images of a pGEMEX-1 obtained at 1 fps. The elapsed time is shown in each image. Scale bar, 200 nm. (B) DNA strands were traced in 20 successive frames and the traced images were overlaid. Fast-scanning direction (parallel to *x*-axis) and slow scanning direction (parallel to *y*-axis) are shown by blue and red arrows, respectively. (C) Analytical image; DNA was fitted by the vectors. The angle of theta was calculated as inner product of the vectors. (D) Probability distributions of bending energy: red, green and blue lines are 3, 2, and 1 fps, respectively. (For interpretation of the references to colour in this figure legend, the reader is referred to the web version of this article.)

probe has little effect and that the observed time-dependent change of DNA is mainly owing to thermal Brownian motion.

Focusing on the DNA segments, which exhibit marked fluctuations different from those of the pinned segment, the elastic bending energy, which is one of the parameters that features DNA conformations, is estimated by analyzing the bending motion. We defined the vectors as depicted in Fig. 1C. The length of the vector is about 30 nm, which is less than the persistence length of DNA (50 nm). The elastic bending energy of DNA is calculated as follows:

$$E_{bend} = \sum \kappa(1-\cos\theta_i) = \sum \kappa(1-\vec{r}_i \cdot \vec{r}_{i+1}/|\vec{r}_i||\vec{r}_{i+1}|)$$

where $\kappa/k_BT \approx l_p \approx 50$; l_p is the persistence length (50 nm).

We calculated elastic bending energies every 5 s and averaged them. Fig. 1D shows the probability distribution of bending energy, where the red, green, and blue lines are at 3, 2, and 1 fps, respectively. All lines are almost coincident, and fluctuations are also the same. This indicates that thermal energy is essentially the same during the thermal motions for the period between 1 and 3 fps. In other words, we may mention that there is no injection of thermal energy originating from the scanning motion of the AFM probe. From the above consideration, at least in the experimental conditions given in this study, we conclude that DNA conformations are independent of AFM scanning in this case.

3.2. AFM imaging of poly-nucleosomal arrays

An AFM image in air of the poly-nucleosomal array reconstituted by the salt-dialysis procedure depicts a typical "beads-on-a-string structure" (Fig. 2A). Note that the prepared sample was not treated with any cross-linkers such as glutaraldehyde. The collection of images illustrates the nature of this type of specimen; the number of the nucleosome formed on a DNA strand varied between 1 and 6, and the contour length of the nucleosomal arrays (from one end of the DNA strand to the other end) was dependent on the number of nucleosomes formed on the DNA. The calculated decrement of the contour length was ~50 nm (~149 bp) per nucleosome particle formation (Fig. 2B).

DNA templates containing a set of nucleosome-positioning sequences, such as 5S rDNA or 601 sequences, have been frequently used in the structural and functional analysis of nucleosome [40,41]. The benefit of utilizing these sequences is

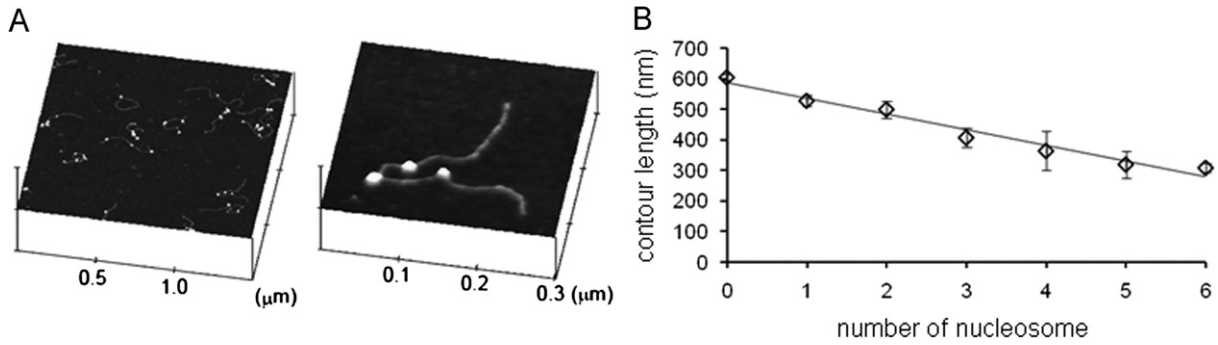

Fig. 2. Reconstitution of nucleosomal array on linearized DNA. (A) An example of AFM image of nucleosomal array reconstituted from purified core histone and linear plasmid DNA (1890 bp). Enlarged image is shown (right). (B) Relationship between the contour length of the reconstituted nucleosomal array and the number of nucleosomes formed on the array. Data were collected from 50 individual images.

the stable formation of nucleosomes on the desired position. However, we avoided using such positioning signals because it restricts the dynamics of natural histone–DNA interaction.

3.2.1. Nucleosome movement along the DNA

Now the fast-scanning AFM was applied to analyze the nucleosome dynamics in solution (Fig. 3A). At t=0, five nucleosomes were found on this array. For convenience, these five nucleosomes were termed *N1*, *N2*, *N3*, *N4*, and *N5*. Accordingly, the DNA fragments separated by the nucleosomes *N1–N5* were designated as l_1–l_6 as shown in the figure. The motion of DNA strand and the positions of the nucleosomes were traced every 2 s up to 20 s and are overlaid in Fig. 3B. In this example, the linker DNA segments between *N4–N5*, and between *N5* and its closer DNA end, were relatively stable. On the other hand, the other fragments were mobile and showed swinging motions.

With regard to the nucleosome movements, some nucleosomes (*N4* and *N5*) stably stayed at the same positions on the mica, whereas other nucleosomes (*N1*, *N2*, and *N3*) appeared to keep changing their positions with some restrictions (Fig. 3B). These observations indicate that the movement of nucleosomes on the mica surface is restricted and not free from interaction between the core histone and the mica. At least some nucleosomes seemed to slide along the DNA with restrictions and therefore change the x–y positions on the mica surface. Other nucleosomes apparently did not move along the DNA strand except for small fluctuations. When the contour length of the linker DNA (between nucleosomes) was measured over time (Fig. 3C), this situation becomes clearer. The measurement of l_1 showed a sudden increase in 5.0–5.5 s. The shortening of l_2 was coincidentally observed at the same time. The degrees of these increase and decrease were about 23 and 27 nm in l_1 and l_2, respectively, corresponding to the difference of the mean values from 5 s before and after the change. The sum of l_1 and l_2 did not show any changes during the observation (Fig. S2), indicating that nucleosome *N1* slid along the DNA towards nucleosome *N2*, while nucleosome *N2* did not change its position on the DNA.

The length of l_4 suddenly increased from 10.5 to 11.5 s. At the same time, both l_5 and l_6 did not change. Therefore, the increase of l_4 must be caused by a dynamic movement of N_3. Unfortunately, the length of l_3 showed a relatively large fluctuation, and, thus, it was not possible to analyze the l_3 dynamics in detail.

The results described above are the first visual evidence that the histone core particles slide along the DNA without the help of other protein factors. The range of nucleosome movement sheds significant insight on the sliding mechanisms. In our experiment, the histone core particle slid along the DNA by a distance of 31.9 ± 12.0 nm on average, ranging from 22.7 to 45.5 nm, and a successive long-range nucleosome movement was not observed. This value is smaller than the length of nucleosomal DNA (50 nm, ~146 bp). This indicates that even if sliding occurs, only a part of the nucleosomal DNA can be converted to free DNA, and the other part is still in contact with the core histone particle.

In the present study, the nucleosome sliding occurred within a few seconds or less. This time scale is very close to that of unwrapping–rewrapping event observed in single-molecule FRET experiments [23,24]. It has been shown that wrapping–unwrapping of DNA is an intrinsic property of nucleosome, and, nucleosomes are partially unwrapped about 2–10% of the time [23]. It has also been shown that nucleosome with only one turn of DNA is so unstable that nucleosomes either wrap more DNA or dissociate [22,42]. All these results indicate that nucleosome structure itself is intrinsically negotiable (stable but with a flexibility of partial unwrapping and sliding), rather than fixed and uniform. The sliding of nucleosome may be a stochastic phenomenon caused by a manifestation of the dynamic properties of nucleosomal DNA induced by thermal fluctuation.

3.2.2. Histone release from nucleosome array

In addition to nucleosome sliding, nucleosome disruption can also be observed by fast-scanning AFM. Fig. 4A illustrates a histone core particle dissociation from a tri-nucleosomal array. Initially, three nucleosomes were on the DNA template. At t=21.0, histone core particle (indicated by arrow) was released from the DNA. The volumes of the nucleosome core particles (Fig. 4B) on the DNA and the core histone octamer dissociated from the DNA were 530.4 ± 45.0 and 207.5 ± 19.3 nm^3 (Fig. 4B and D), respectively, demonstrating a real nucleosome disruption. The contour lengths of this nucleosomal array before (650.3 ± 16.1 nm) and after (699.0 ± 6.8 nm) this event also support the disruption (Fig. 4B). It is interesting to note that, although this dissociation process occurred within 1 s, a gradual increase of the contour length was observed from 19.5 to 21.5 s. It seems to take some time for the nucleosomal DNA that has lost the core histone to completely relax.

Fig. 4C shows another type of nucleosome disruption. A single nucleosome was observed in the initial image and stably imaged until 119.0 s. At 121.0 s, the core particle was split into two small particles. One of them was released from DNA, and the other remained on the DNA until 122.0 s. Two dissociated particles were seen on the mica surface at 124.0 s. The volume of the dissociated particle (83.7 ± 16.0 nm^3) was about a half of the volume of free histone core particle (207.5 ± 19.3 nm^3), indicating that the core particle dissociated into its constituent subunits.

Our results described in Fig. 4 clearly demonstrated that nucleosome disassembly occurred at least under two distinct

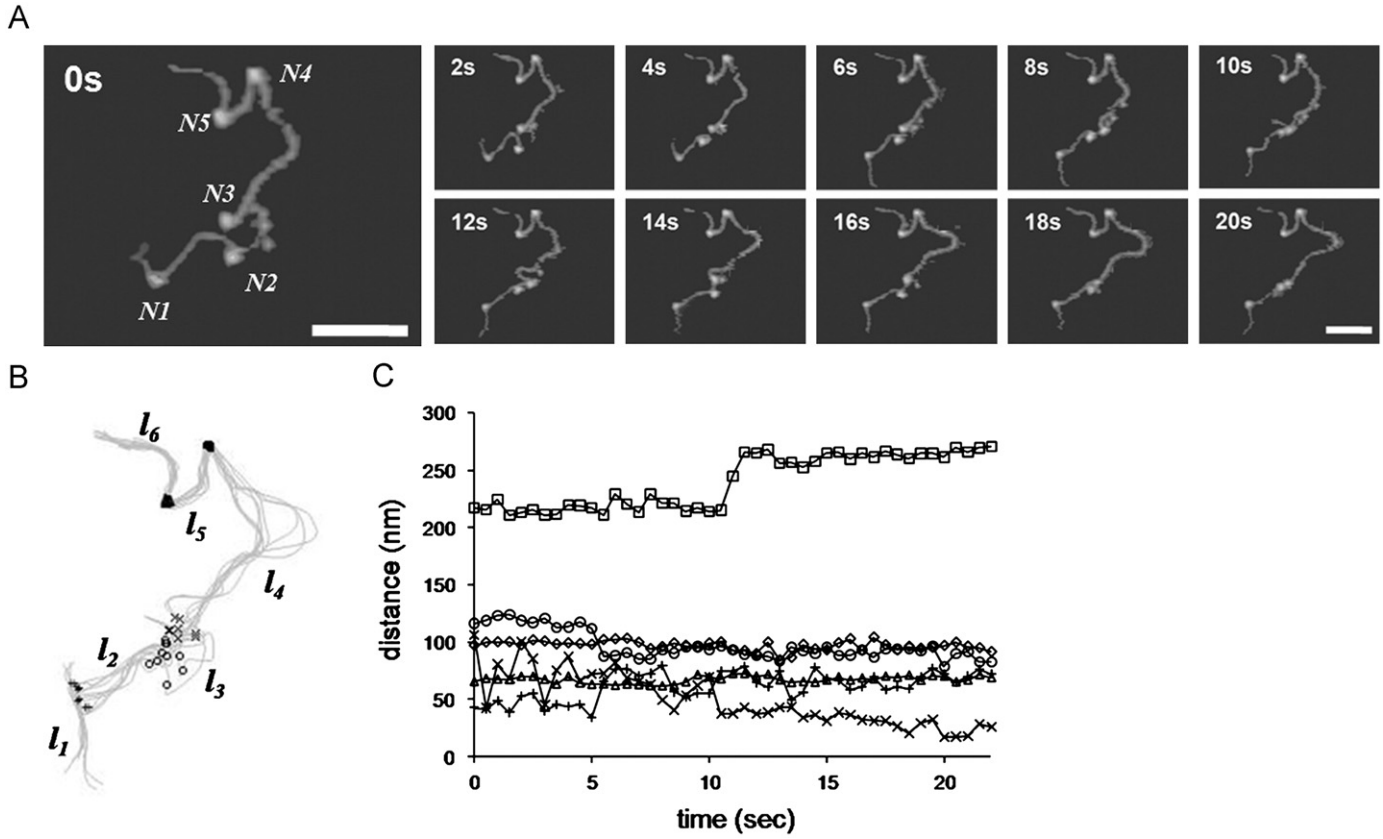

Fig. 3. Fast-scanning AFM analysis of nucleosome dynamics. (A) Time-lapse images of a reconstituted nucleosomal array obtained at 2 fps. Images of every 2.0 s are selected and sorted (the elapsed time is shown in each image). The images were trimmed from the original scan size of 800 × 600 nm^2. Scale bar—100 nm. (B) Movement of nucleosomes on mica. The DNA chain of the nucleosomal array was traced every 2.0 s and overlaid. The center of five nucleosomes (*N1* (+), *N2* (○), *N3* (×), *N4* (□), *N5* (△)) are indicated. (C) Changes in the DNA length between adjacent nucleosomes (or nucleosome and the closer end of DNA) over a time period of 22 s; l_1 (between *N1* and the closer end of DNA), l_2 (between *N1* and *N2*), l_3 (between *N2* and *N3*), l_4 (between *N3* and *N4*), l_5 (between *N4* and *N5*), and l_6 (between *N5* and the closer end of DNA) are indicated by (+), (○), (×), (□), (△), and (◇), respectively.

mechanisms: (i) all the core histones are released from DNA at once under the current limited-time resolution (0.5 s per frame) and (ii) histone subunits sequentially dissociate from nucleosome. Based on our observation, the second step in the latter case occurs within a few seconds after the first step, whereas the first step rarely occurs even within 100 s. Hence, it is likely that the second step of the disassembly occurs much faster than the first step, and that the intermediate state of disruption (between the first and second steps) is very unstable and easily proceeds to the completely dissociated state.

A detailed analysis of the dissociated particles in the sequential disassembly demonstrated that the volume of the released particles was approximately a half of that of a histone octamer (Fig. 4), suggesting that a tetramer is the unit of the released histones. Although it is difficult to clarify which subunit(s) of core histone dissociate(s) in the first step and second step, there are several issues to be considered. It has been shown biochemically that the subunit composition of nucleosome can be changed, resulting in different "nucleosomes" coexisting in a chromatin fiber [43–45]. The H2A–H2B dimer more easily dissociates from nucleosome than the H3–H4 tetramer [45,46]. Therefore, histone disassembly has been believed to be achieved by the initial release of two histone H2A–H2B dimers, and subsequent disruption of the $(H3–H4)_2$ tetramer into two H3–H4 dimers [43]. The recent recognition imaging technique has enabled an analysis of the nucleosome remodeling process and demonstrated that partially disrupted nucleosomes lacking one H2A–H2B dimer or two H2A–H2B dimers co-exist with the intact ones on the nucleosome array [47]. Alternatively, since the histone core particle is formed by binding of two histone H2A–H2B dimers to each side of the histone $(H3–H4)_2$ tetramer, it may be possible that a sequential release of two H2A–H2B dimers results in an instantaneous formation of $(H2A–H2B)_2$ tetramer, or one possible constituent of the released tetramers could be (H3–H4)–(H2A–H2B). At present, there are technical difficulties to prove the components of the released particle. However the sequential dissociation observed by AFM will likely provide new insight on the mechanisms of nucleosome remodeling and a foundation for future investigations.

4. Conclusion

This study demonstrates the ability of fast-scanning AFM to investigate DNA and nucleosome dynamics in solution. The analysis of plasmid DNA movement showed that there is no influence of the tip motion on the DNA dynamics. Therefore the observed movement of DNA is caused mainly by thermal fluctuation of the environment. This feature of the experimental system allowed us to investigate dynamical properties of nucleosomes. When the dynamics of "beads-on-a-string" was analyzed, the nucleosome sliding (fluctuation) was observed within the range of ~50 nm. In addition to sliding, nucleosome disruption was also observed. Nucleosome collapses into core histone and DNA in two different ways: one is the octamer release and the other the possible sequential subunits release. All of these processes were completed within a few seconds. These successful applications of fast-scanning AFM to the analysis of nucleosome dynamics will provide a foundation for future investigations and open the possibility that dynamics in biological reaction might be

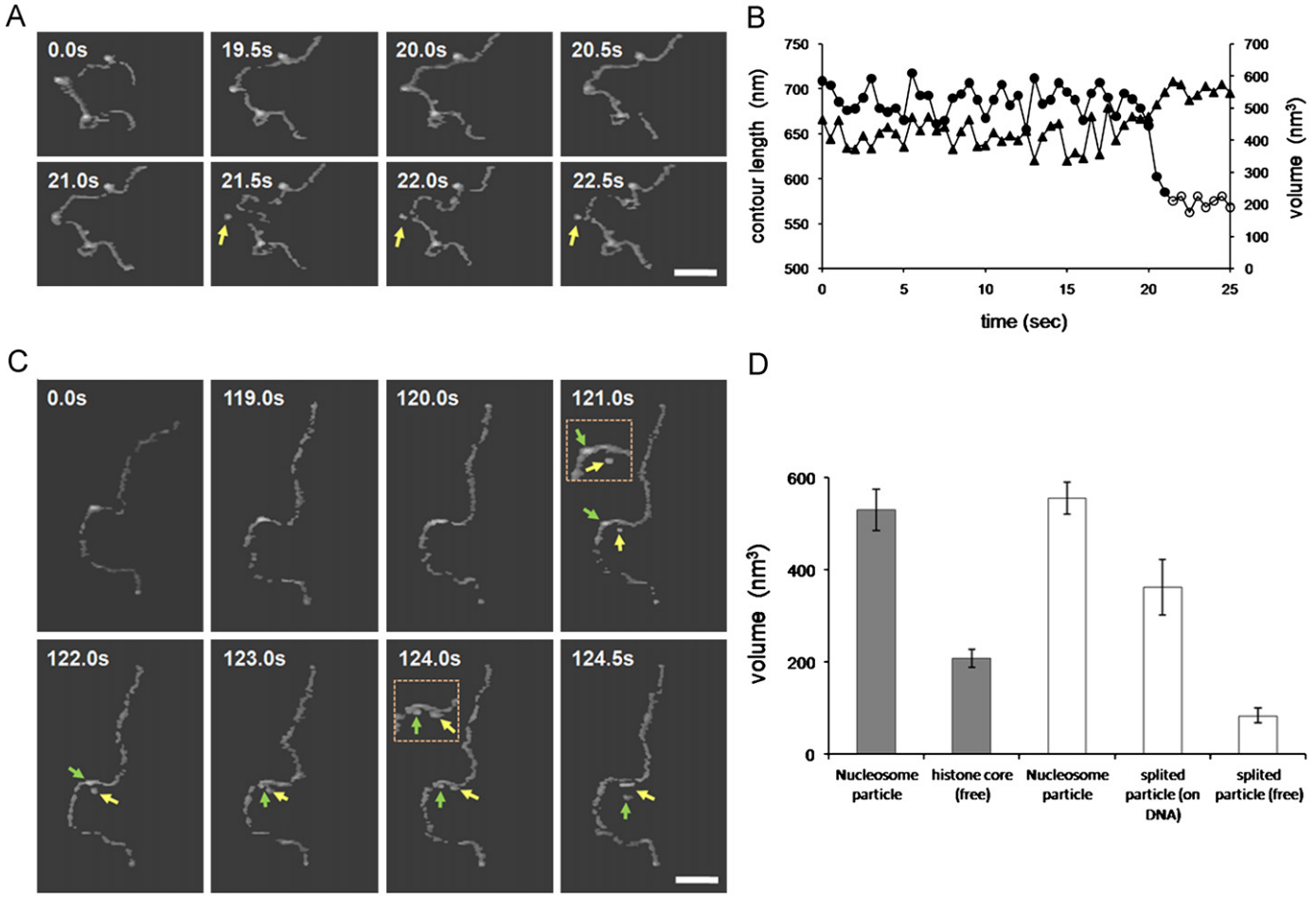

Fig. 4. Dissociation of core histone from nucleosome array (A and C). Time-lapse images of reconstituted nucleosomal array were obtained at 2 fps. Dissociated particles are indicated by arrows. Scale bar—100 nm. (B) The contour lengths of the nucleosomal array (▲) and the volumes of nucleosome particle on the array (●) were measured every 0.5 s and plotted. The volumes of dissociated particle after t=21.5 s are shown in open circles (○). Data from (A) were used in (B). In (C), the nucleosome core particle was split into two particles (arrows). (D) The volumes of the nucleosome core and the dissociated histone particles were measured and histogramed. Data in (A) and (C) were used and summarized in filled and open bars, respectively.

imaged with previously unattainable temporal and spatial resolution.

Acknowledgements

This work was supported by grants from the Japanese Ministry of Education, Culture, Sports, Science, and Technology (Grant-in-Aid for Scientific Research on Priority Areas to K.T., S.H.Y., and K.Y.), from Japan Society for the Promotion of Science (Grant-in-Aid for Basic Research (A) to K.T., Young Scientists (B) to K.H.), by the Inamori Foundation (to K.H.), and by SENTAN, JST (Japan Science and Technology Agency). Y.S. is a recipient of the JSPS (Japan Society for the Promotion of Science) predoctoral fellowship.

Appendix A. Supplementary material

Supplementary data associated with this article can be found in the online version at doi:10.1016/j.ultramic.2010.02.032.

References

[1] M. Fixman, J. Kovac, J. Chem. Phys. 58 (1973) 1564–1568.
[2] P.J. Hagerman, Annu. Rev. Biophys. Biophys. Chem. 17 (1988) 265–286.
[3] S.H. Yoshimura, C. Yoshida, K. Igarashi, K. Takeyasu, J. Electron Microsc. (Tokyo) 49 (2000) 407–413.
[4] T. Yanao, K. Yoshikawa, Phys. Rev. E Stat. Nonlin. Soft Matter Phys. 77 (2008) 021904.
[5] T. Ohta, S. Nettikadan, F. Tokumasu, H. Ideno, Y. Abe, M. Kuroda, H. Hayashi K. Takeyasu, Biochem. Biophys. Res. Commun. 226 (1996) 730–734.
[6] K. van Holde, J. Zlatanova, Bioessays 16 (1994) 59–68.
[7] K.J. Scanlon, Y. Ohta, H. Ishida, H. Kijima, T. Ohkawa, A. Kaminski, J. Tsai G. Horng, M. Kashani-Sabet, FASEB J. 9 (1995) 1288–1296.
[8] S.E. Halford, A.J. Welsh, M.D. Szczelkun, Annu. Rev. Biophys. Biomol. Struct. 33 (2004) 1–24.
[9] S.C. Kowalczykowski, D.A. Dixon, A.K. Eggleston, S.D. Lauder, W.M. Rehrauer, Microbiol. Rev. 58 (1994) 401–465.
[10] S.H. Yoshimura, R.L. Ohniwa, M.H. Sato, F. Matsunaga, G. Kobayashi, H. Uga C. Wada, K. Takeyasu, Biochemistry 39 (2000) 9139–9145.
[11] R.D. Kornberg, Science 184 (1974) 868–871.
[12] P. Oudet, M. Gross-Bellard, P. Chambon, Cell 4 (1975) 281–300.
[13] K. Luger, A.W. Mader, R.K. Richmond, D.F. Sargent, T.J. Richmond, Nature 389 (1997) 251–260.
[14] T.E. O'Neill, M. Roberge, E.M. Bradbury, J. Mol. Biol. 223 (1992) 67–78.
[15] J.D. Anderson, J. Widom, J. Mol. Biol. 296 (2000) 979–987.
[16] K.J. Polach, J. Widom, J. Mol. Biol. 254 (1995) 130–149.
[17] G. Meersseman, S. Pennings, E.M. Bradbury, EMBO J. 11 (1992) 2951–2959.
[18] S. Pennings, G. Meersseman, E.M. Bradbury, J. Mol. Biol. 220 (1991) 101–110.
[19] S. Pennings, G. Meersseman, E.M. Bradbury, Proc. Natl. Acad. Sci. USA 91 (1994) 10275–10279.
[20] T. Sakaue, K. Yoshikawa, S.H. Yoshimura, K. Takeyasu, Phys. Rev. Lett. 87 (2001) 078105.
[21] B.D. Brower-Toland, C.L. Smith, R.C. Yeh, J.T. Lis, C.L. Peterson, M.D. Wang, Proc. Natl. Acad. Sci. USA 99 (2002) 1960–1965.
[22] S. Mihardja, A.J. Spakowitz, Y. Zhang, C. Bustamante, Proc. Natl. Acad. Sci. USA 103 (2006) 15871–15876.

[23] G. Li, M. Levitus, C. Bustamante, J. Widom, Nat. Struct. Mol. Biol. 12 (2005) 46–53.
[24] H.S. Tims, J. Widom, Methods 41 (2007) 296–303.
[25] T. Berge, D.J. Ellis, D.T. Dryden, J.M. Edwardson, R.M. Henderson, Biophys. J. 79 (2000) 479–484.
[26] D.J. Ellis, D.T. Dryden, T. Berge, J.M. Edwardson, R.M. Henderson, Nat. Struct. Biol. 6 (1999) 15–17.
[27] M. Guthold, M. Bezanilla, D.A. Erie, B. Jenkins, H.G. Hansma, C. Bustamante, Proc. Natl. Acad. Sci. USA 91 (1994) 12927–12931.
[28] M. Guthold, X. Zhu, C. Rivetti, G. Yang, N.H. Thomson, S. Kasas, H.G. Hansma, B. Smith, P.K. Hansma, C. Bustamante, Biophys. J. 77 (1999) 2284–2294.
[29] S. Kasas, N.H. Thomson, B.L. Smith, H.G. Hansma, X. Zhu, M. Guthold, C. Bustamante, E.T. Kool, M. Kashlev, P.K. Hansma, Biochemistry 36 (1997) 461–468.
[30] T. Ando, N. Kodera, E. Takai, D. Maruyama, K. Saito, A. Toda, Proc. Natl. Acad. Sci. USA 98 (2001) 12468–12472.
[31] N. Crampton, M. Yokokawa, D.T. Dryden, J.M. Edwardson, D.N. Rao K. Takeyasu, S.H. Yoshimura, R.M. Henderson, Proc. Natl. Acad. Sci. USA 104 (2007) 12755–12760.
[32] M. Kobayashi, K. Sumitomo, K. Torimitsu, Ultramicroscopy 107 (2007) 184–190.
[33] M. Yokokawa, C. Wada, T. Ando, N. Sakai, A. Yagi, S.H. Yoshimura, K. Takeyasu, EMBO J. 25 (2006) 4567–4576.
[34] K. Hizume, T. Nakai, S. Araki, E. Prieto, K. Yoshikawa, K. Takeyasu, Ultramicroscopy 109 (2009) 868–873.
[35] M. de Frutos, E. Raspaud, A. Leforestier, F. Livolant, Biophys J. 81 (2001) 1127–1132.
[36] K. Hizume, S. Araki, K. Yoshikawa, K. Takeyasu, Nucleic Acids Res. 35 (2007) 2787–2799.
[37] K. Hizume, S.H. Yoshimura, K. Takeyasu, Biochemistry 44 (2005) 12978–12989.
[38] M.H. Sato, K. Ura, K.I. Hohmura, F. Tokumasu, S.H. Yoshimura, F. Hanaoka K. Takeyasu, FEBS Lett. 452 (1999) 267–271.
[39] R.M. Henderson, S. Schneider, Q. Li, D. Hornby, S.J. White, H. Oberleithner, Proc. Natl. Acad. Sci. USA 93 (1996) 8756–8760.
[40] P.T. Lowary, J. Widom, J. Mol. Biol. 276 (1998) 19–42.
[41] R.T. Simpson, F. Thoma, J.M. Brubaker, Cell 42 (1985) 799–808.
[42] L.S. Shlyakhtenko, A.Y. Lushnikov, Y.L. Lyubchenko, Biochemistry 48 (2009) 7842–7848.
[43] M. Eitoku, L. Sato, T. Senda, M. Horikoshi, Cell. Mol. Life Sci. 65 (2008) 414–444.
[44] R.T. Kamakaka, S. Biggins, Genes Dev. 19 (2005) 295–310.
[45] F. Thoma, DNA Repair (Amsterdam) 4 (2005) 855–869.
[46] A. Wunsch, V. Jackson, Biochemistry 44 (2005) 16351–16364.
[47] R. Bash, H. Wang, C. Anderson, J. Yodh, G. Hager, S.M. Lindsay, D. Lohr, FEBS Lett. 580 (2006) 4757–4761.